DTIC FILE COPY

AD____________

AD-A223 389

MODELING OF THE NON-AUDITORY RESPONSE TO BLAST OVERPRESSURE

Use of Surrogate and Analytical Models to Understand the Parameters Controlling Blast Injury to the Gastro-intestinal Tract

ANNUAL/FINAL REPORT

James H. Stuhmiller
James H.-Y. Yu
Edward J. Vasel

JANUARY 1990

Supported by

U.S. ARMY MEDICAL RESEARCH AND DEVELOPMENT COMMAND
Fort Detrick, Frederick, Maryland 21701-5012

Contract No. DAMD17-85-C-5238

JAYCOR
11011 Torreyana Road
San Diego, California 92121-1190

Approved for public release; distribution unlimited

The findings in this report are not to be construed as an official Department of the Army position unless so designated by other authorized documents.

1990

90 07 2 031

MODELING OF THE NON-AUDITORY RESPONSE TO BLAST OVERPRESSURE

Use of Surrogate and Analytical Models to Understand the Parameters Controlling Blast Injury to the Gastro-intestinal Tract

JANUARY 1990

Supported by

U.S. ARMY MEDICAL RESEARCH
AND DEVELOPMENT COMMAND
Fort Detrick
Frederick, Maryland 21701-5012

Contract No. DAMD17-85-C-5238

UNCLASSIFIED
SECURITY CLASSIFICATION OF THIS PAGE

REPORT DOCUMENTATION PAGE

1a. REPORT SECURITY CLASSIFICATION Unclassified	1b. RESTRICTIVE MARKINGS N/A
2a. SECURITY CLASSIFICATION AUTHORITY N/A	3. DISTRIBUTION / AVAILABILITY OF REPORT Approved for Public Release; Distribution unlimited
2b. DECLASSIFICATION / DOWNGRADING SCHEDULE N/A	
4. PERFORMING ORGANIZATION REPORT NUMBER(S)	5. MONITORING ORGANIZATION REPORT NUMBER(S)
6a. NAME OF PERFORMING ORGANIZATION JAYCOR Applied Sci. & Engr. Technol. Group 6b. OFFICE SYMBOL (If applicable)	7a. NAME OF MONITORING ORGANIZATION Director Walter Reed Army Institute of Research
6c. ADDRESS (City, State, and ZIP Code) 11011 Torreyana Rd. San Diego, CA 92121-1190	7b. ADDRESS (City, State, and ZIP Code) ATTN: SGRD-UWZ-C, Kenneth T. Dodd, Ph.D. Bldg. 40 Washington, DC 20307-5100
8a. NAME OF FUNDING / SPONSORING ORGANIZATION U. S. Army Medical Res. & Devel. Cmd. 8b. OFFICE SYMBOL (If applicable)	9. PROCUREMENT INSTRUMENT IDENTIFICATION NUMBER DAMD17-85-C-5238
8c. ADDRESS (City, State, and ZIP Code) Fort Detrick Frederick, MD 21701-5012	10. SOURCE OF FUNDING NUMBERS

PROGRAM ELEMENT NO.	PROJECT NO.	TASK NO.	WORK UNIT ACCESSION NO.
62787A	62787A878	AB	004

11. TITLE (Include Security Classification)

(U) Modeling of the Non-Auditory Response to Blast Overpressure

12. PERSONAL AUTHOR(S) James H. Stuhmiller, James H.-Y. Yu, and Edward J. Vasel

13a. TYPE OF REPORT	13b. TIME COVERED	14. DATE OF REPORT (Year, Month, Day)	15. PAGE COUNT
Annual/Final	FROM 8/15/85 TO 7/31/89	1990 January	30

16. SUPPLEMENTARY NOTATION
Use of Surrogate and Analytical Models to Understand the Parameters Controlling Blast Injury to the Gastro-intestinal Tract

17. COSATI CODES		
FIELD	GROUP	SUB-GROUP
26	14	
23	04	

18. SUBJECT TERMS (Continue on reverse if necessary and identify by block number)
RA 3, Weapons Effects (Biological), Non-Auditory Responses, Blast Overpressure, Explosions, G.I. tract, Blast Injuries (JG)

19. ABSTRACT (Continue on reverse if necessary and identify by block number)

Previous experimental studies using excised, perfused rabbit intestine in a sealed water tank, have provided direct visual observation that air bubbles produce local, violent, intestinal wall motion when they collapse under blast loading and that injury directly correlates with those motions. Measurements of the pressure within the bubble was shown to correlate with the motion of the wall and with injury. It was speculated that this pressure is an indirect measure of the stress in the wall tissue and therefore could be a means of quantifying the injury process.

An analytical model of the dynamics of a bubble within an elastic membrane has been developed. Surrogate models, using materials with properties similar to that of intestine wall, but arranged in simpler geometric configurations, have been used to collect data on the dynamic process. The model results are compared and discussed.

20. DISTRIBUTION / AVAILABILITY OF ABSTRACT ☐ UNCLASSIFIED/UNLIMITED ☒ SAME AS RPT. ☐ DTIC USERS	21. ABSTRACT SECURITY CLASSIFICATION Unclassified
22a. NAME OF RESPONSIBLE INDIVIDUAL Mary Frances Bostian	22b. TELEPHONE (Include Area Code) [301] 663-7325 22c. OFFICE SYMBOL SGRD-RMI-S

DD FORM 1473, 84 MAR

SECURITY CLASSIFICATION OF THIS PAGE
UNCLASSIFIED

19. ABSTRACT *(Continued from front)*

USE OF SURROGATE AND ANALYTICAL MODELS TO UNDERSTAND THE PARAMETERS CONTROLLING BLAST INJURY TO THE GASTRO-INTESTINAL TRACT

James H. Stuhmiller, Ph.D.
Vice President, Engineering Services Group
James H.-Y. Yu, Ph.D.
Manager, Engineering Mechanics Laboratories
Edward J. Vasel
Senior Scientist, Engineering Mechanics Laboratories
JAYCOR

ABSTRACT

Previous experimental studies using excised, perfused rabbit intestine in a sealed water tank, have provided direct visual observation that air bubbles produce local, violent, intestinal wall motion when they collapse under blast loading and that injury directly correlates with those motions. Measurements of the pressure within the bubble was shown to correlate with the motion of the wall and with injury. It was speculated that this pressure is an indirect measure of the stress in the wall tissue and therefore could be a means of quantifying the injury process.

An analytical model of the dynamics of a bubble within an elastic membrane has been developed. Surrogate models, using materials with properties similar to that of intestine wall, but arranged in simpler geometric configurations, have been used to collect data on the dynamic process. The model results are compared and discussed.

Accession For
NTIS GRA&I
DTIC TAB
Unannounced
Justification

DTIC
COPY
INSPECTED
5

A-1

CONTENTS

Page

ABSTRACT

1. INTRODUCTION 1

2. SURROGATE EXPERIMENTS 3

3. ANALYTICAL MODEL 5
   Dynamics of the Liquid Motion 5
   Dynamics of the Bubble Motion 7
   Geometric Parameterization 7
   Liquid Pressure Field 9
   Numerical Solution Algorithm 10

4. MODEL VALIDATION 11
   Parameter Assignments 11
   Discussion of Results 11

5. CONCLUSIONS 17

6. REFERENCES 19

ILLUSTRATIONS

Figure		Page
1.	Schematic of single curvature membrane test fixture	4
2.	Comparison of calculation and measurement of bubble pressure time histories	12
3.	Comparison of calculation and measurement of bubble pressure extrema parameters for the conditions shown in Figure 2	13
4.	Comparison of measured and calculated bubble pressure time histories for cases when the membrane has positive and negative curvatures	15
5.	Comparison of calculated differential pressure time histories for positive and negative curvature of the membrane	16
6.	Comparison of calculated and measured differential pressure maximum values	16

1. INTRODUCTION

Injury to the gastro-intestinal tract is one of the primary biological effects of strong blast exposure. The threshold for injury appears to lie between that for the larynx and the lung and therefore may be a critical element in defining Damage Risk Criteria for occupational exposure. In combat circumstances, this injury may be debilitating.

Little is known about the mechanics of the injury process or its relation to external blast characteristics. In fact, little is known about the pressure environment within the abdomen during blast loading. Laboratory experiments at JAYCOR using perfused, small animal intestine have provided most of our current understanding of the phenomena [1].

In those tests, the static bursting strength of various sections of rabbit intestine were determined. There seems to be little systematic variation with location along the gastro-intestinal tract or with animal weight, age, or sex. The material properties were in agreement with Yamada [2]. The most prevalent form of injury is hemorrhage without associated rupture, so that it is likely that threshold injury is controlled by the failure of the vascular system.

Dynamic experiments were then conducted in which isolated sections of intestine were placed in a water filled chamber and exposed to an external blast loading. Damage to the intestine could be directly correlated with the location of air bubbles within the section. Violent motion of the tissue was observed and, during the overexpansion phase, rupture sometimes occurred.

Tests made with balloons filled with air and water and immersed in water produced a similar dynamic response. High speed movies showed surface deformations that were primarily limited to the local region at the bubble. As the viscosity of the interior fluid was increased, the deformations became even more localized. Pressure probes placed inside the bubble showed that the surface motion could be correlated with the variations in the pressure time histories. This correlation suggested that bubble pressure measurements could be used to understand the injury process.

Interpretation of the observed damage in isolated intestine sections was clouded by the differences from the in vivo situation. The lack of a blood supply causes the intestine to deteriorate rapidly and, of course, eliminates the possibility of observing hemorrhage.

A surgical technique was developed by Yu and Vasel that allowed an isolated rabbit intestine to be oxygenated by the animal's own cardiopulmonary system. The perfusion results from connecting the abdominal aorta to the cranial mesenteric artery and connecting the portal vein to the caudal vena cava. The intestine can be maintained in a nearly in vivo state while being subjected to blast loading in a water chamber.

Results obtained with the previous isolated preparation were confirmed and thresholds of hemorrhagic injury at lower levels were observed. Occurrence of injury was not completely correlated with the peak chamber pressure, however, suggesting that local conditions were important.

Direct measurement of the stress in the wall section proved to interfere with the dynamical motion and a noninvasive technique was sought. Pressure transducers placed within the bubble showed the same behavior as had been observed in the isolated preparations. Moreover, the pressure differential between the bubble and a position in the fluid near the bubble seemed to correlate better with injury.

As a result of these findings, a relation between air bubbles and injury was proposed. The pressure differential across the membrane gives a measure of the dynamics, hence the stress in the tissue. An analogy was drawn with the relation between surface tension and pressure difference in a bubble. The amount of test data on which this concept is based is small, however, and there are many uncontrolled factors in dealing with the entire gastro-intestinal tract. A simpler circumstance was sought in which to develop and test these ideas.

2. SURROGATE EXPERIMENTS

The objective of the experiments is to provide data on gas and lumen dynamics under controlled circumstances so that the hypotheses proposed can be tested. At the same time, we want to perfect techniques for measuring the tissue dynamics that can be used in future animal tests.

Lamb cecum sections, in a commercially available and preserved form, were used as the surrogate material. Tests were run to demonstrate that they had material strengths comparable to that of rabbit intestine. A fixture was designed to be placed in the water chamber, holding the section at a circular ring. The fixture formed an enclosure surrounding the membrane with flow holes at the side. See Figure 1. By adjusting the volume of water and gas under the membrane, the curvature could be varied continuously from convex to concave and the bubble could be given any volume.

Pressure probes were mounted at fixed locations on either side of the initial membrane position. Pressure measurements were also taken in the chamber, away from the fixture.

As the intensity of the blast was increased, as measured by the peak chamber pressure, the maximum pressure reached inside the bubble and the frequency of bubble oscillation increased.

The differential pressure between the inside and outside probes also increased with intensity. For positively curved membranes (bubble on the concave side) the differential pressure first goes negative before rising to its positive maximum. For negative curvature (bubble on the convex side), the curve reverses in sign. Rupture of the membrane usually occurred in this case.

The differential pressure maximum did not vary significantly with the size of the bubble, but it decreased as the membrane was stretched flatter. The differential pressure also decreased as the initial bubble pressure was increased.

These observations form a basis on which to develop and test the analytical model discussed in the next section.

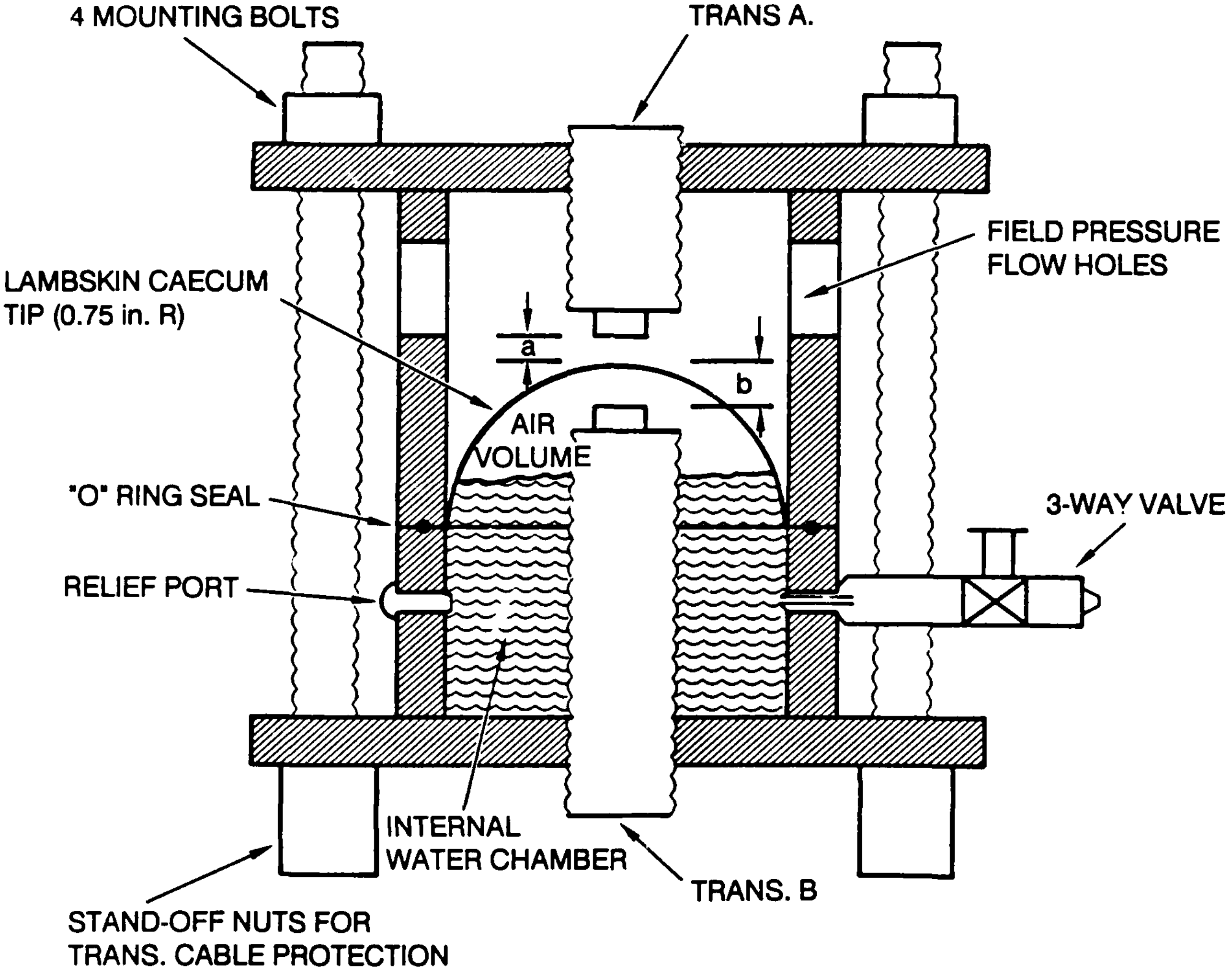

Figure 1. Schematic of single curvature membrane test fixture.

3. ANALYTICAL MODEL

DYNAMICS OF THE LIQUID MOTION

We use the statement of energy conservation to develop a dynamical equation of motion. The rate of change of kinetic energy in the liquid outside the membrane, E, is equal to the work done by pressure forces at the interface and at the far boundaries less the rate at which energy is dissipated within the liquid flow.

$$\frac{dE}{dt} = (pAv)_i - (pAv)_B - \alpha E \tag{1}$$

where the kinetic energy is given by

$$E = \iiint \frac{1}{2} \rho_L v^2 \, dV \quad . \tag{2}$$

A dissipation rate proportional to the kinetic energy, as occurs in turbulent flow, has been assumed. The pressure at the interface on the liquid side is equal to the pressure in the gas, p_G, less the differential pressure caused by the tension in membrane, δp_M,

$$p_i = p_G - \delta p_M \quad . \tag{3}$$

The contribution of the membrane depends on its material properties and its deformation.

We imagine a coordinate system based on the liquid in which one coordinate direction, x, is parallel everywhere to the flow. The flow area normal to the coordinate x is designated A(x). The liquid velocity is then always normal to A so that the statement of mass conservation becomes

$$\rho_L \, v(x) \, A(x) = \text{constant} \quad . \tag{4}$$

Since the liquid is assumed to be incompressible and since the geometries must be conformal to the membrane position, then

$$v(x) \, A(x) = v_i A_i \tag{5}$$

The differential volume in this coordinate system is given by

$$dV = A \, dx \quad . \tag{6}$$

Combining the above relations gives

$$E = \int_{x_i}^{x_B} \frac{1}{2} \rho_L \left[\frac{v_i A_i}{A}\right]^2 A dx$$

$$= \frac{1}{2} \rho_L (v_i A_i)^2 \int_{x_i}^{x_B} \frac{dx}{A(x)} \quad . \tag{7}$$

The rate of change of the energy is then

$$\frac{dE}{dt} = \rho_L (v_i A_i) \frac{d}{dt} (v_i A_i) \int_{x_i}^{x_B} \frac{dx}{A(x)} + \frac{1}{2} \rho_L (v_i A_i)^2 \frac{d}{dt} \int_{x_i}^{x_B} \frac{dx}{A(x)}$$

$$= \rho_L (v_i A_i) \frac{d}{dt} (v_i A_i) \int_{x_i}^{x_B} \frac{dx}{A(x)} + \frac{1}{2} \rho_L (v_i A_i)^2 \left(- \frac{v_i}{A_i}\right)$$

$$= \rho_L (v_i A_i) \left[\int_{x_i}^{x_B} \frac{dx}{A(x)} \cdot \frac{d}{dt} (v_i A_i) - \frac{1}{2} v_i^2 \right] \quad . \tag{8}$$

The rate of change of the volume flux is

$$\frac{d}{dt} (v_i A_i) = A_i \frac{dv_i}{dt} + v_i \frac{dA_i}{dt}$$

$$= A_i \frac{dv_i}{dt} + v_i \left(\frac{dA}{dx}\right)_i \frac{dx_i}{dt}$$

$$= A_i \frac{dv_i}{dt} + v_i^2 \left(\frac{dA}{dx}\right)_i \tag{9}$$

Combining (7)-(9) with (1) yields the equation of motion

$$I \frac{dv_i}{dt} + R v_i^2 = (p_G - \delta p_M - p_B)/\rho_L - \alpha I v_i \tag{10}$$

where p_B is the applied pressure at the far boundary and the inertia and kinematic coefficients are given by

$$I = A_i \int_{x_i}^{x_B} \frac{dx}{A(x)} \tag{11}$$

$$R = \left(\frac{dA}{dx}\right)_i \int_{x_i}^{x_B} \frac{dx}{A(x)} - \frac{1}{2} \quad . \tag{12}$$

DYNAMICS OF THE BUBBLE MOTION

The rate of change of the bubble volume is equal to the volume flux in the liquid

$$\frac{dV_b}{dt} = A_i v_i \tag{13}$$

since the liquid is incompressible. Because the blast loadings are so rapid, we assume that process is adiabatic within the bubble so that for an ideal gas

$$p_G V_b^\gamma = p_G(0)\ V_b^\gamma(0) \quad . \tag{14}$$

Finally, the pressure differential due to the membrane must be found from experiment. For an elastic material

$$\delta p_M = \delta p_M(A_b) \quad . \tag{15}$$

GEOMETRIC PARAMETERIZATION

Various flow geometries can be simulated through the choice of V(x). For example, a spherical bubble in an infinite medium would be characterized by

$$V(x) = \frac{4}{3} \pi x^3 \tag{16}$$

$$x_B = \infty \quad . \tag{17}$$

Using (6), (11), and (12) yields

$$A(x) = 4\pi x^2$$

$$I = x$$

$$R = \frac{3}{2}$$

which produces Rayleigh's equation [3]

$$x \frac{dv}{dt} + \frac{3}{2} v^2 = \frac{p_G - p_\infty}{\rho_L} \quad . \tag{18}$$

Similarly, a plug of water of radius r and length L yields

$$V(x) = \pi r^2 x \tag{19}$$

$$x_B = x_i + r \tag{20}$$

so that

$$A(x) = \pi r^2$$

$$I = L$$

$$R = -\frac{1}{2}$$

and the dynamical equation

$$L \frac{dv_i}{dt} - \frac{1}{2} v_i^2 = \frac{p_a - p_L}{\rho_L} \quad . \tag{21}$$

For the surrogate experiments described earlier, the appropriate geometry is a spherical sector anchored at a ring of radius r_1 with an outer boundary at a radius r_2. Then

$$V(x) = \frac{\pi}{6} x \left(3r_1^2 + x^2\right) \tag{22}$$

$$X_B = r_2 \tag{23}$$

which yields

$$A(x) = \frac{\pi}{2} \left(r_1^2 + x^2\right)$$

$$I = \frac{r_1^2 + x^2}{r_1} \left[\tan^{-1}\left(\frac{r_2}{r_1}\right) - \tan^{-1}\left(\frac{x}{r_1}\right)\right]$$

$$R = \frac{2x}{r_1} \left[\tan^{-1}\left(\frac{r_2}{r_1}\right) - \tan^{-1}\left(\frac{x}{r_1}\right)\right] \quad .$$

LIQUID PRESSURE FIELD

Because the surrogate experiments collected pressure data at points within the liquid it is desirable to form an expression for the pressure field. If the previous derivation were carried out for a region of liquid bound by x and x_B, then we would have found

$$\int_{x_i}^{x_B} \frac{dx}{A(x)} \frac{d}{dt} (\rho_L vA) = (p - p_B) + \frac{1}{2} \rho_L v^2 \quad . \tag{24}$$

Using (5) and rearranging the left-hand side of (24) yields

$$\frac{d}{A(x)} I(x) \frac{d}{dt} (\rho_L v_i A_i) = (p - p_B) + \frac{1}{2} \rho_L v^2 \quad , \tag{25}$$

while the same form at the interface is

$$\frac{1}{A_i} I_1 \frac{d}{dt} (\rho_L v_i A_i) = (p_G - \delta p_M - p_B) + \frac{1}{2} \rho v_i^2 \quad . \tag{26}$$

Taking the ratio of (25) and (26) and solving for p yields

$$p(x) = p_B - \frac{1}{2} \rho_L v^2 + \left(p_G - \delta p_M - p_B + \frac{1}{2} \rho_L v_i^2\right) \left[\frac{A_i I(x)}{A(x) I_i}\right] \quad . \tag{27}$$

NUMERICAL SOLUTION ALGORITHM

The set of coupled ordinary differential equations for the position and velocity of the membrane coordinate is solved by a fifth-order Runge-Kutta algorithm [4]. Time steps were taken to be 0.05 msec and variations were made to assure that accurate solutions were being obtained.

4. MODEL VALIDATION

PARAMETER ASSIGNMENTS

For the surrogate test fixture described earlier, the following geometric parameters apply. The 5 cc bubble forms a spherical section with base radius of 1.68 cm and height 1.00 cm. Based on the previous experimental observations, we assume that the membrane distorts only in the region of the bubble and maintains the geometry of a spherical section. The partly enclosed fixture has an effective radius of 1.91 cm as measured from the bubble center. We then can use the geometry described by (22) and (23) with the values

$$r_1 = 1.68 \text{ cm}$$

$$r_2 = 1.91 \text{ cm}$$

$$x(0) = 1.00 \text{ cm}$$

The differential pressure in the membrane is taken from tests data to increase at a rate of 3 psi/cm. The flow is assumed to have no damping.

For the negative curvature runs, we have

$$r_1 = 1.91 \text{ cm}$$

$$r_2 = 1.91 \text{ cm}$$

$$x(0) = -1.91 \text{ cm}$$

The chamber pressure is taken from the measured trace for each shot and is characterized by a peak value and duration to the first zero crossing. The durations varied from 4.4 to 5.0 ms.

DISCUSSION OF RESULTS

Figure 2 compares the bubble pressure time histories for a series of tests in which the chamber pressured varied from 27 to 116 psig. The plots are not to scale so only shape can be compared here. There seems to be generally good agreement on the number and shape of peaks. The increasing oscillation frequency with blast intensity is captured.

Figure 3 shows the quantitative comparison of these results. The decrease with intensity of the time between peaks is accurately predicted by the model as is the first maximum and minimum in the trace. At high intensities, the calculation tends to over predict the second and third maxima.

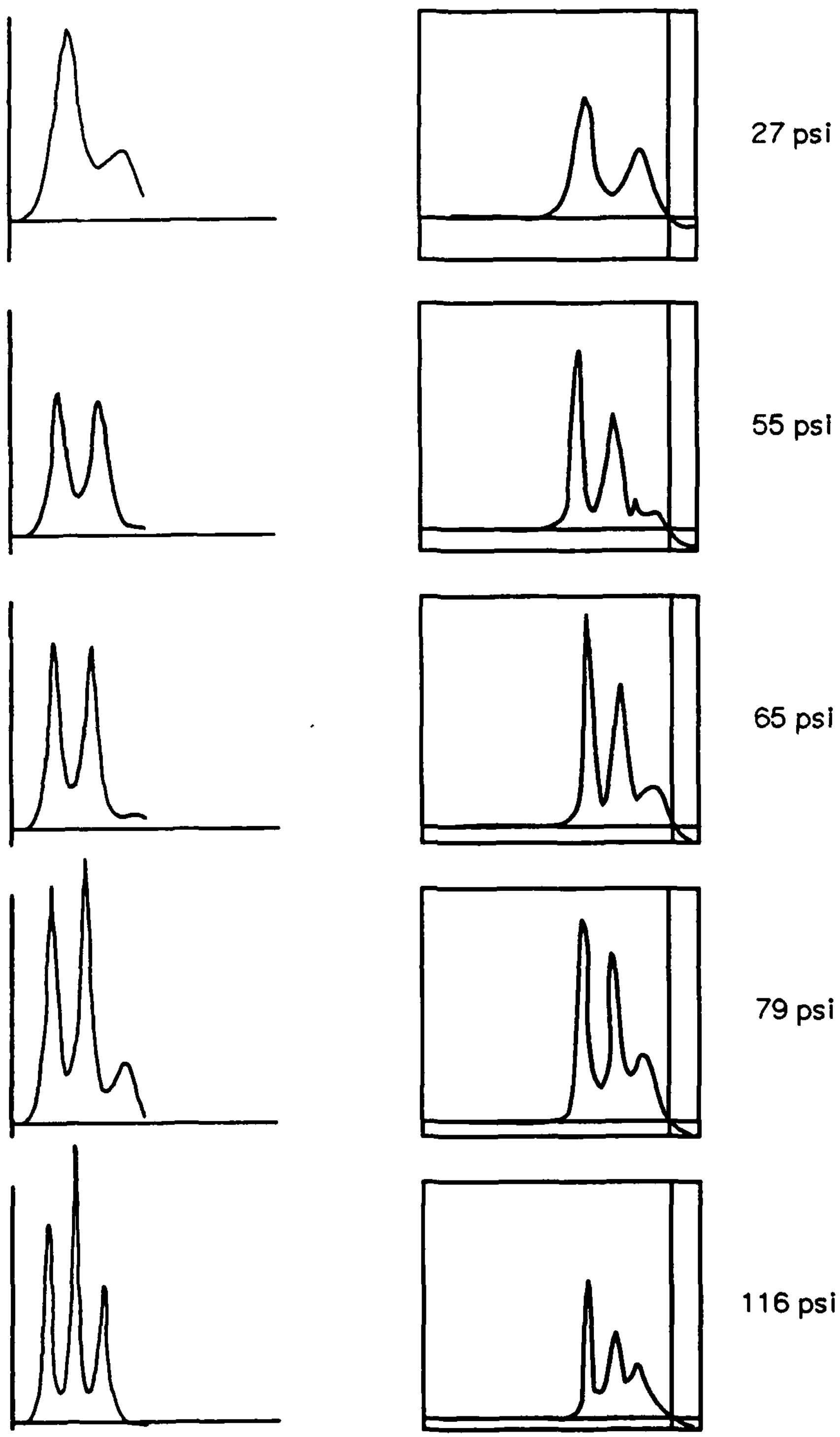

Figure 2. Comparison of calculation and measurement of bubble pressure time histories. Membrane has positive curvature with a bubble volume of 5 cc. Axes are not to scale so only shape can be compared.

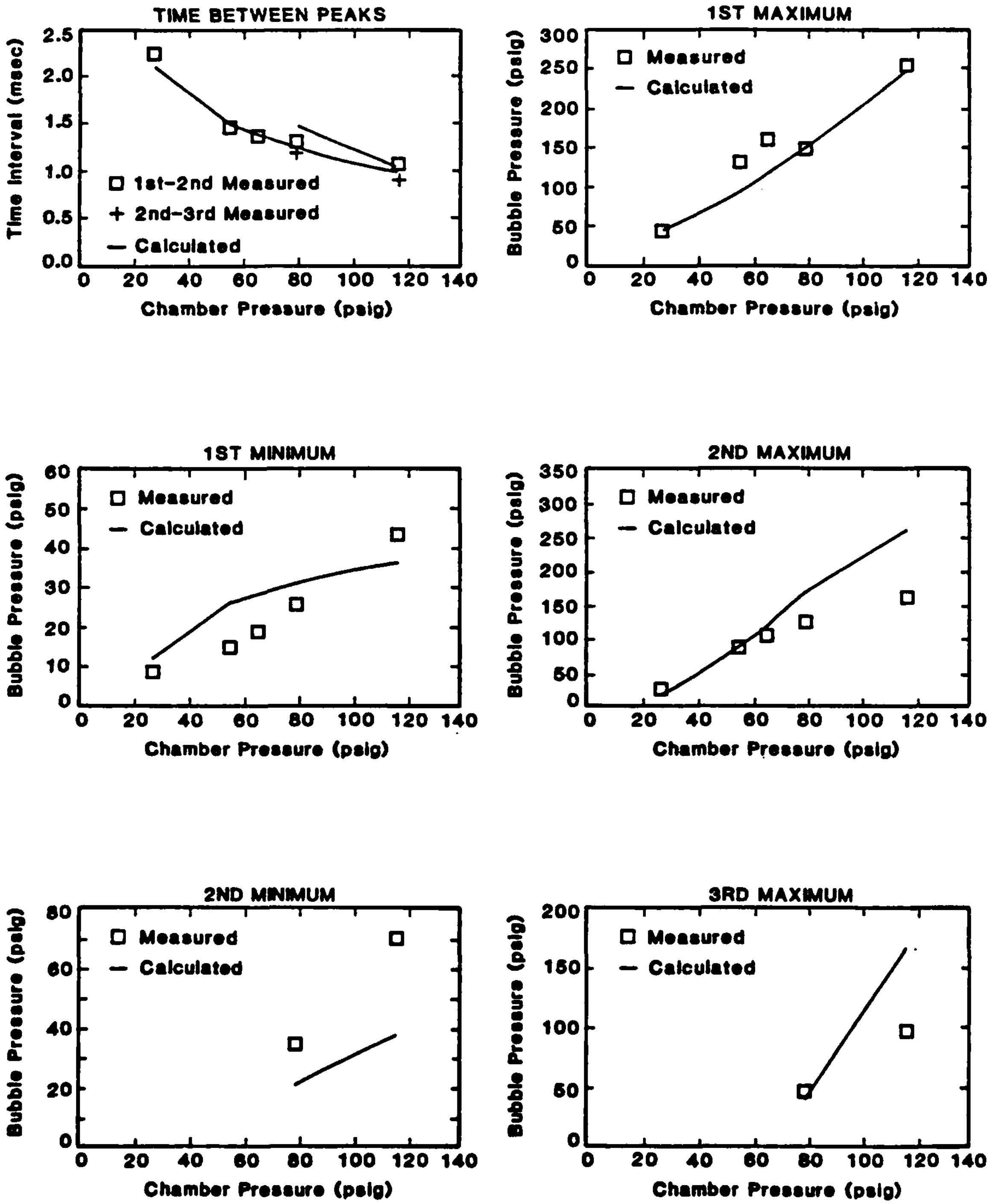

Figure 3. Comparison of calculation and measurement of bubble pressure extrema parameters for the conditions shown in Figure 2.

A review of the experimental data revealed that the membrane struck the inside transducer in these cases. The impact may have slowed the collapse process and caused a smaller peak to be reached.

Figure 4 compares the bubble pressure time histories for the cases of positive and negative curvature in the membrane. The change in frequency is captured. Figure 5 shows the calculated pressure differential between the inside and outside transducers. The dramatic reversal of the trace reported in the experimental data is seen. Figure 6 presents the comparison of the calculated and measured pressure differential maximum values. Agreement is only qualitative in this case. Again, the impact with the inner transducer may have affected the results. However, both 5 and 10 cc bubbles produced nearly the same differential pressures, confirming the experimental observations.

The predicted bubble responses did not vary significantly with the assumed stiffness of the membrane for the range of values measured, indicating that the pressure differentials are primarily controlled by the flow dynamics in the water. Another evidence of this dependence was that the response, especially the pressure differential, varied with the assumed flow geometry.

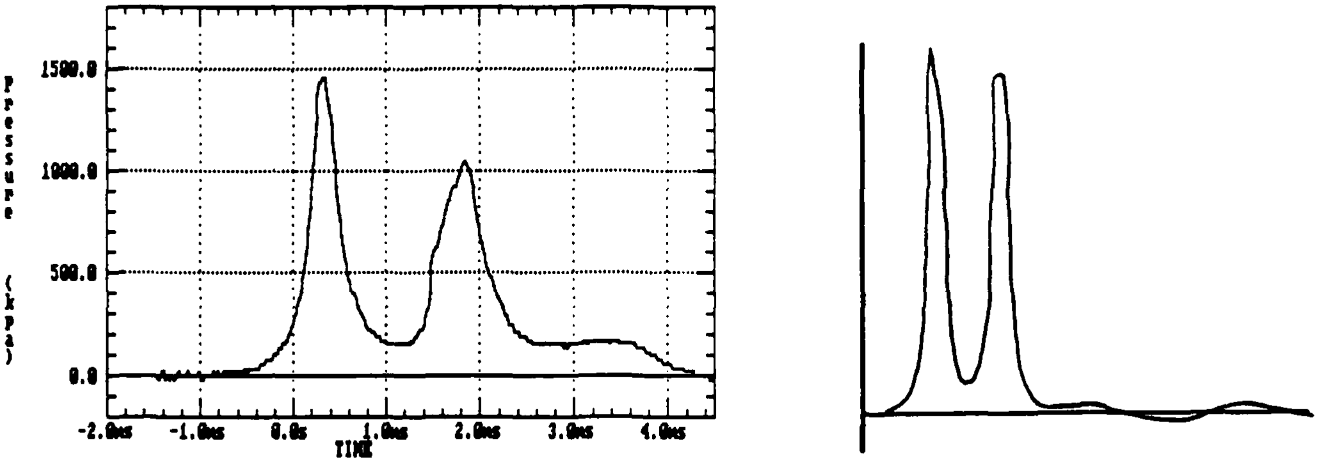

Measured

Calculated

Positive Curvature

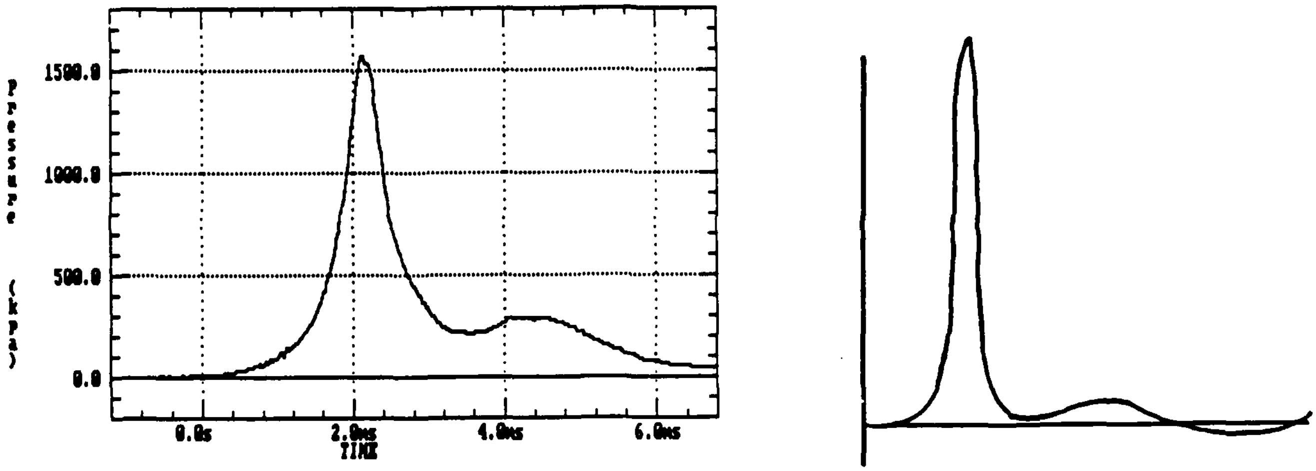

Measured

Calculated

Negative Curvature

Figure 4. Comparison of measured and calculated bubble pressure time histories for cases when the membrane has positive and negative curvatures.

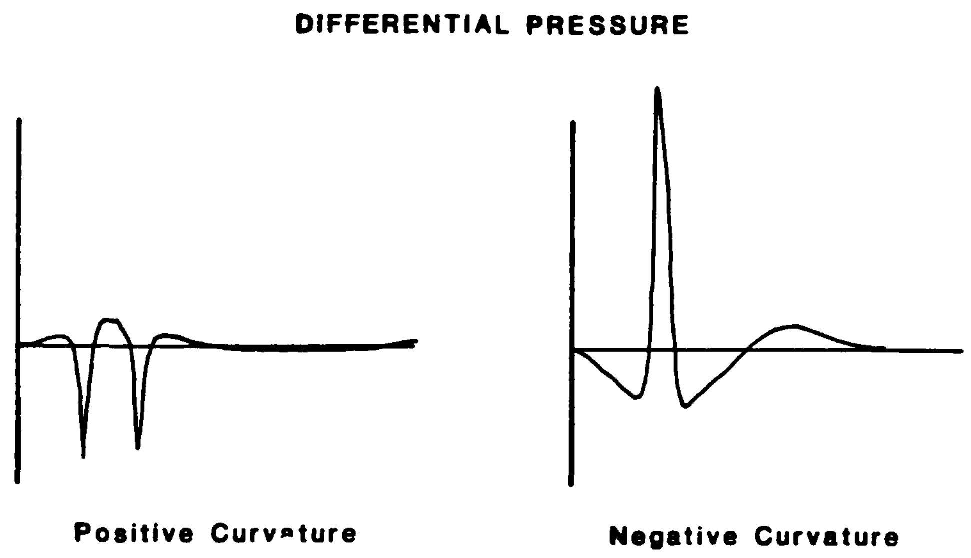

Figure 5. Comparison of calculated differential pressure time histories for positive and negative curvature of the membrane.

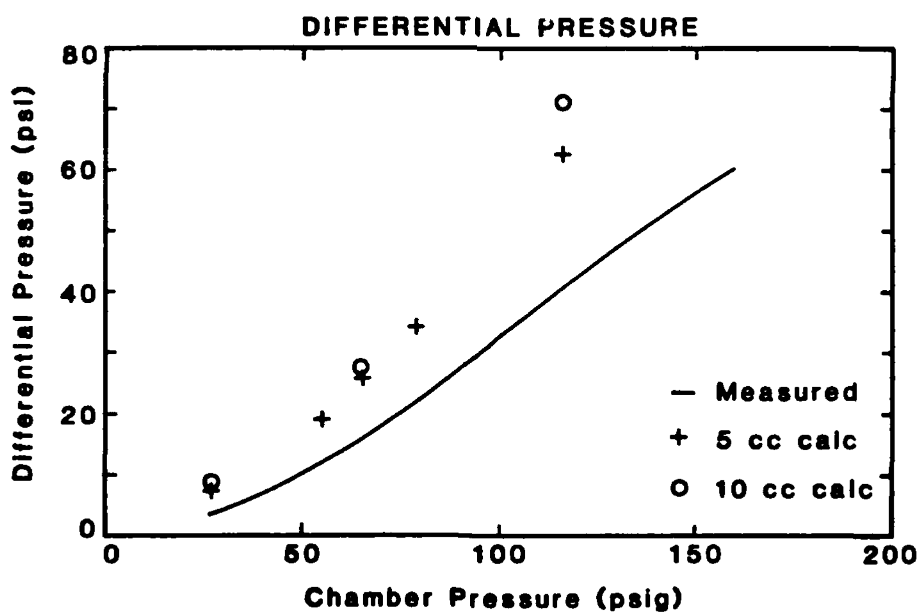

Figure 6. Comparison of calculated and measured differential pressure maximum values.

5. CONCLUSIONS

The analytical model provides a reasonably good explanation of the observed dynamics of the bubble. In future tests, it will be used to predict the response in a complex wave environment and to anticipate membrane rupture. Eventually, these concepts will be employed in developing an understanding of the mechanisms of gastro-intestinal injury in vivo.

6. REFERENCES

1. J. H.-Y. Yu and E. J. Vasel, "Experimental study of the correlation between gastro-intestinal injury and blast loading," Final Report for Contract DAMD17-83-C-3221, U.S. Army Medical Research and Development Command, Fort Detrick, Frederick, Md., December 1984.

2. H. Yamada, Strength of Biological Materials, edited by F. G. Evans, Williams & Williams, Baltimore, Md., 1970.

3. H. Lamb, Hydrodynamics, Cambridge University Press, §91, 1932.

4. J. Todd, Survey of Numerical Analysis, McGraw-Hill, §2.28, 1962.

DISTRIBUTION LIST

4 copies	Director Walter Reed Army Institute of Research ATTN: SGRD-UWZ-C Washington, DC 20307-5100
1 copy	Commander US Army Medical Research and Development Command ATTN: SGRD-RMI-S Fort Detrick, Frederick, MD 21701-5012
2 copies	Defense Technical Information Center (DTIC) ATTN: DTIC-DDAC Cameron Station Alexandria, VA 22304-6145
1 copy	Dean School of Medicine Uniformed Services University of the Health Sciences 4301 Jones Bridge Road Bethesda, MD 20814-4799
1 copy	Commandant Academy of Health Sciences, US Army ATTN: AHS-CDM Fort Sam Houston, TX 78234-6100